

RESEARCH  
PAPER



# Around the world in 10 million years: biogeography of the nearly cosmopolitan true toads (Anura: Bufonidae)

Jennifer B. Pramuk<sup>1\*</sup>, Tasia Robertson<sup>2</sup>, Jack W. Sites Jr<sup>2</sup> and Brice P. Noonan<sup>3</sup>

<sup>1</sup>Department of Herpetology, Bronx Zoo/  
Wildlife Conservation Society, 2300 Southern  
Boulevard, Bronx, NY 10460, USA,

<sup>2</sup>Brigham Young University, Department of  
Integrative Biology, Provo, UT 84602, USA,

<sup>3</sup>Duke University, Department of Biology,  
Durham, NC 27708, USA

## ABSTRACT

**Aim** The species-rich family of true toads (Anura: Bufonidae) has been the focus of several earlier studies investigating the biogeography of geographically widespread taxa. Herein, we employ newly developed Bayesian divergence estimate methods to investigate the biogeographical history of this group. Resulting age estimates are used to test several key temporal hypotheses including that the origin of the bufonid clade pre-dates Gondwanan vicariance (~105 million years ago, Ma). Area cladograms are also invoked to investigate the geographical origin of the family.

**Location** Worldwide, except the Australia–New Guinea plate, Madagascar and the Antarctic.

**Methods** A phylogenetic hypothesis of the relationships among true toads was derived from analysis of 2521 bp of DNA data including fragments from three mitochondrial (*12S*, *tRNA<sup>val</sup>*, *16S*) and two nuclear (*RAG-1*, *CXCR-4*) genes. Analysis of multiple, unlinked loci with a Bayesian method for estimating divergence times allowed us to address the timing and biogeographical history of Bufonidae. Resulting divergence estimates permitted the investigation of alternative vicariance/dispersal scenarios that have been proposed for true toads.

**Results** Our area cladogram resulting from phylogenetic analysis of DNA data supports a South American origin for Bufonidae. Divergence estimates indicate that the family originated earlier than had been suggested previously (78–99 Ma). The age of the enigmatic Caribbean clade was dated to the late Palaeocene–early Eocene. A return of bufonids to the New World in the Eocene was followed by rapid diversification and secondary expansion into South America by the early Oligocene (Rupelian).

**Main conclusions** The South American origin of Bufonidae in the Upper Cretaceous was followed by relatively rapid expansion and radiation around the globe, ending with a return to the Americas via a Eurasian/North American land bridge in the Eocene. Though the exact route of this dispersal (Beringia or North Atlantic) remains unclear, an argument is made for the less frequently invoked North Atlantic connection. The origin of the enigmatic Caribbean lineage was found to be consistent with colonization following the bolide impact at the K/T boundary. These findings provide the first, firm foundation for understanding true toad divergence times and their truly remarkable and global radiation.

## Keywords

Anura, Bayes method, biogeography, Bufonidae, *CXCR-4*, divergence times, DNA, mtDNA, phylogeny, *RAG-1*, South America.

\*Correspondence: Jennifer Pramuk, Curator of Herpetology, Bronx Zoo/Wildlife Conservation Society, Bronx, NY 10460, USA. E-mail: jpramuk@wcs.org

## INTRODUCTION

One fundamental goal of modern systematics investigations is to use the resulting phylogenies to help understand global

biogeographical patterns. Once a well-supported phylogenetic framework is accomplished, it can be employed to estimate divergence times to arrive at an overall picture of the spatial and temporal biogeographical framework of a taxonomic group.

Members of the species-rich true toad family Bufonidae, comprising *c.* 481 species (<http://amphibiaweb.org>), are native to most regions of the world except the Australia–New Guinea plate, Madagascar and the Antarctic. Their broad geographical distribution has prompted a great many studies focused on resolving the evolutionary relationships of bufonid frogs (e.g. Blair, 1972; Maxson, 1984; Graybeal, 1997; Pauly *et al.*, 2004; Frost *et al.*, 2006; Pramuk, 2006), however, the limited fossil record of this group has provided few calibration points and therefore prevented most workers from estimating divergence times to investigate their age and correlated biogeography. To explain the modern day distribution of true toads, several distinct biogeographical hypotheses proposing various combinations of vicariance and intercontinental dispersal events have been invoked. For example, earlier hypothetical origins for Bufonidae (reviewed in Pauly *et al.*, 2004) range from an African (Tihen, 1962) to a South American origin (Blair, 1972; Maxson, 1984) with hypothesized dispersal and/or vicariance events explaining their modern day, nearly cosmopolitan distribution. Most recently, Pramuk (2006) hypothesized that her phylogeny for Bufonidae, derived from molecular and morphological data, is consistent with an origin that pre-dates Gondwanan vicariance (>105 million years ago, Ma). Similarly, earlier studies offered a Gondwanan vicariance scenario to explain the biogeographical patterns present in this family (e.g. Savage, 1973; Maxson, 1984). Here, we employ phylogenetic reconstruction methods and Bayesian analyses of divergence ages to compare general hypotheses of the spatial and temporal origin of Bufonidae.

The data set of Pramuk (2006), containing 3.5 kb of nuclear and mitochondrial data sequenced for 109 individuals, is currently the most complete for investigating relationships within what formerly was referred to as ‘*Bufo*’. Prior to Frost *et al.* (2006), the vast majority of species assigned to Bufonidae were placed in the genus *Bufo*; however, these authors elevated most intrageneric clades to new genera. Except where noted, we provisionally adopt the taxonomy proposed by Frost *et al.* (2006).

To test spatial and temporal hypotheses of Bufonidae, we employ the data set of Pramuk (2006) and combine it with novel sequences from an additional nuclear marker (the exon *CXCR-4*), to make it compatible with a previously published data set (Biju & Bossuyt, 2003). Moreover, by expanding the outgroup sampling we increased the number of fossil calibration points in our analysis that fall outside of the fossil-poor Bufonidae. Our resulting maximum parsimony (MP), maximum likelihood (ML) and Bayesian topologies are broadly congruent with those of earlier studies (Frost *et al.*, 2006; Pramuk, 2006) but they differ in a few notable ways from the former study; the differences between our results and the biogeographical implications of these temporally referenced patterns are discussed herein.

## METHODS

### Taxon sampling

To obtain a strongly supported hypothesis of relationships within Bufonidae, a previously analysed data matrix of *c.* 2821 bp

of *12S–16S* mtDNA and *RAG-1* nuclear data (Pramuk, 2006) for 89 terminals was expanded by the addition of 750 bp of the nuclear exon *CXCR-4*. To provide additional distant Neobatrachian and Archaeobatrachian outgroups, and hence calibration points outside of Bufonidae for divergence time analysis, we included this nuclear marker to make our matrix compatible with that of Biju & Bossuyt (2003), which included homologous sequence data for 2521 bp of *12S* and *16S* rRNA, *RAG-1* and *CXCR-4*. In total, new sequences were collected for 89 specimens representing 74 species, including data for 70 bufonids and four outgroup taxa.

To resolve a phylogeny of Bufonidae, genes with disparate rates of evolutionary change were sequenced to target a wide range of signal and to incorporate independently evolving molecular markers (Pennington, 1996). For example, regions of the *12S–16S* mitochondrial genome were sequenced to give signal at intermediate and recent levels of divergence. The *12S–16S* fragment was obtained with several sets of overlapping primers used previously for *Bufo* (Goebel *et al.*, 1999; Pramuk, 2006) or modified from published primers. Portions of the nuclear *RAG-1* and *CXCR-4* exons were sequenced in order to provide signal at deeper levels of divergence and were selected based on their established phylogenetic utility for other groups of vertebrates (e.g. Biju & Bossuyt, 2003). All primers used in this study, and their original references, are listed in Table 1.

### DNA extraction, polymerase chain reaction amplification and DNA sequencing

Previously published data for the *12S–16S* fragment (Pauly *et al.*, 2004) were used for the outgroups *Ceratophrys cornuta* and *Hyla cinerea*. Additionally, previously published sequences (Biju & Bossuyt, 2003) for *CXCR-4* and portions of *12S* and *16S* rRNA data were included for 31 additional outgroup taxa. For a complete list of voucher specimens and their respective GenBank accession numbers, refer to Appendix S1 in Supplementary Material.

Prior to extraction, tissues were stored at  $-80^{\circ}\text{C}$  or fixed in 95–100% ethanol. The DNA was extracted from small amounts (*c.* 50 ng) of muscle or liver tissue with the Qiagen DNeasy Tissue Kit<sup>®</sup> and visualized on 1% high melt agarose gels in Tris–acetate–EDTA (TAE) buffer. We performed a polymerase chain reaction (PCR) in 13- $\mu\text{l}$  reactions containing TaKaRa Hotstart *Taq* polymerase, 10 $\times$  reaction buffer [100 mM Tris HCl (pH 8.3), 500 mM KCl, 15 mM MgCl<sub>2</sub>]. Amplification followed published PCR conditions and was performed on a MJ Research thermal cycler. Cycle sequencing reactions were completed with Big Dye Sequencing kits (ABI Inc.). The PCR products were purified with Millipore MANU030 PCR plates. Double-stranded, purified products were used in 1/32 deoxy-termination sequencing reactions (10  $\mu\text{l}$  total volume). Sequencing reactions were cleaned with Sephadex columns and sequencing was performed directly using an ABI 3100 automated sequencer.

The program Sequencher 3.1.1 (Gene Codes Corp.) was used to edit sequences. CLUSTALX (Thompson *et al.*, 1997) was employed to perform preliminary alignment using default parameters (gap opening = 15; gap extension = 6.666; delay

**Table 1** Amplification and sequencing primers used for the continuous *12S–16S* region of the mitochondrial genome, and portions of the nuclear genes *CXCR-4* and *RAG-1*. Position refers to the location of the *12S–16S* rRNA primers in the *Xenopus* mitochondrial genome. The Goebel no. refers to primers listed in Goebel *et al.* (1999; Table 3). *CXCR-4* and *RAG-1* primers are from Biju & Bossuyt (2003) and Chiari *et al.* (2004), respectively. Other modified primers are from Pramuk (2006).

Primer name	Position	Primer sequence (5' → 3')	Goebel no.
12SZL	2206–2225	AAAGGTTTGGTCCTAGCCTT	35
12H2(R) mod.	2484–2503	GGTATGTAATCCCAGTTTG	N/A
12L6 mod.	2487–2508	ACTGGGATTAGATACCCCACTA	N/A
12SKH	2975–2996	TCCRGTAAYRCTTACCDTGTACGA	70
12Sc(L)	2834–2853	AAGGCGGATTTAGHAGTAAA	65
16H14(R) mod.	3753–3774	TCTTGTTACTAGTTTAAACAT	85
16L10	3622–3641	AGTGGGCCTAAAAGCAGCCA	82
16H10	4054–4076	TGATTACGCTACCTTCGCACGGT	92
16L9	3956–3976	CGCCTGTTTACCAAAAACAT	88
16H13	4551–4572	CCGGTCTGAACTCAGATCACGTA	96
<i>CXCR-4</i> C	–	GTC ATG GGC TAY CAR AAG AA	–
<i>CXCR-4</i> F	–	TGA ATT TGG CCC RAG GAA RGC	–
<i>RAG-1</i> MartFl1	–	AGCTGCAGYCARTAYCAYAARATGTA	–
<i>RAG-1</i> AmpR1	–	AACTCAGCTGCATTKCCAATRTCA	–

divergent sequences = 30%; transition:transversion = 50%), with adjustments by eye. Alignment of the protein coding sequences was straightforward and they were translated into amino acids to verify alignment. Although they were relatively uncommon within nuclear genes, heterozygous bases were coded with IUPAC symbols. Published secondary structure models of the *16S* and *12S* genes for *Eleutherodactylus cuneatus* and *Xenopus laevis* (De Rijk *et al.*, 1994; Van de Peer *et al.*, 1994) were used to infer the secondary structure of the non-protein coding genes. Alignments of ribosomal DNA were adjusted to conform to known secondary structure, and insertions and deletions preferentially were placed into loop regions rather than stems. Regions of the mtDNA that remained unalignable were deleted from analyses using default parameters in the program Gblocks version 0.91b (Castresana, 2000) on the Gblocks server (<http://molevol.ibmb.csic.es/Gblocks.html>).

### Phylogenetic analyses

Maximum parsimony (MP), maximum likelihood (ML) and Bayesian analyses were performed on separate molecular partitions, and were also performed on the combined data sets. Initially, data from each of the three DNA fragments (*12S–16S*, *CXCR-4*, *RAG-1*) were analysed separately. Strong support for individual nodes is defined as nodes with bpp (Bayesian posterior probabilities)  $\geq 0.95$  (Alfaro *et al.*, 2003) or npb (non-parametric bootstrap)  $\geq 70$  (Hillis & Bull, 1993). No strongly supported conflicting relationships were recovered, so all data were combined for subsequent phylogenetic analyses. Maximum parsimony analyses were performed with PAUP\* (version 4.0b10; Swofford, 2002) using a heuristic search with 100 random addition sequence replicates and tree bisection–reconnection (TBR) branch swapping. Nodal support for MP results was assessed through nonparametric bootstrap analysis with 2000 bootstrap pseudoreplicates and 10 random taxon-addition replicates.

The most appropriate model of gene evolution for the ML (and Bayesian) analysis was estimated for each gene region and combined data sets using the Akaike information criterion (AIC)

as implemented in Modeltest 3.06 PPC (Posada & Crandall, 1998). The ML analyses were performed on separate and combined data sets. For ML searches of all combined DNA data, Modeltest selected the best model as GTR + I + G (base frequencies: A, 0.3378; C, 0.2383; G, 0.1701; T, 0.2538; rate matrix: A–C, 1.6291; A–G, 4.7567; A–T, 2.0694; C–G, 1.0174; C–T, 9.5593; G–T, 1.0000; shape parameter for gamma distribution, 0.5244; proportion of invariant sites, 0.2216). The ML searches were run using 100 random addition replicates and TBR branch swapping. Confidence in the resulting topology was assessed with npb (Felsenstein, 1985) with 1000 bootstrap replicates, and heuristic searches of one random addition with TBR branch swapping per replicate.

The data sets were analysed in combined, mixed-model analyses using MrBayes 3.04b (Ronquist & Huelsenbeck, 2003). The analysis of combined data utilized eight model partitions for the *12S–16S*, *RAG-1* and *CXCR-4* data sets (see Table 2 for a summary of each locus). To check for congruence on an identical topology, a minimum of two replicate searches were performed for each separate and combined data set. Analyses were initiated with random starting trees and each analysis was run for  $20 \times 10^6$  generations, with four Markov chains employed and with the chain sampled every 1000th generation. The application Tracer (version 1.2; Rambaut & Drummond, 2003) was used to view output of the *sump* file generated by MrBayes. Trees generated prior to reaching stationarity were discarded as burn-in. Most analyses reached stationarity relatively quickly (all reached stationarity after 160,000 generations).

### Divergence time estimates

We performed divergence time estimates using a relaxed Bayesian molecular clock with uncorrelated rates (BEAST 1.3; Drummond & Rambaut, 2003). This method was chosen over alternatives as recent work has shown that the autocorrelation of rates (e.g. MULTIDIVTIME, Thorne *et al.*, 1998; Thorne & Kishino, 2002) may not be a realistic way to model rate evolution (Drummond *et al.*, 2006). An additional benefit of BEAST is the ability to

Partition (no. of taxa)	No. of characters (pars. inf.)	No. of MP Trees	TL	CI	RI	ML model
12S–16S mtDNA (104)	2023 (955)	804	8662	0.23	0.52	GTR + I + G
RAG-1 (107)	795 (385)	2723	1850	0.48	0.61	TVM + I + G
CXCR-4 (107)	753 (369)	198,052	2606	0.28	0.59	TVM + I + G
All nuclear data (109)	1548 (754)	13,389	4864	0.29	0.58	TVM + I + G
All data (109)	3571 (1709)	1	13,859	0.24	0.54	GTR + I + G

CI, consistency index (excluding uninformative characters); G, gamma; ML, maximum likelihood; MP, most parsimonious; RI, retention index; TL, tree length.

**Table 3** Fourteen calibration points in addition to the root node calibration (employed simultaneously) and their corresponding nodes on our Bayesian tree (Fig. 1).

Calibration (node)	Min. time estimate	Reference
Teleost vs. Tetrapoda (root to tip mean)	420 Ma	San Mauro <i>et al.</i> (2005)
<i>Homo</i> , <i>Gallus</i> (amniotes) vs. amphibians (A)	338 Ma	Ruta <i>et al.</i> (2003)
Divergence of diapsids from synapsids ( <i>Gallus</i> vs. <i>Homo</i> ) (B)	310 Ma	Benton (1997)
Oldest anuran (C) <i>Prosalirus bitis</i>	195 Ma	Jenkins & Shubin (1998)
Oldest discoglossid (F) <i>Eodiscoglossus</i>	164 Ma	Evans <i>et al.</i> (1990)
Origin of Pipoidae (E) <i>Rhadinosteus parvus</i>	151 Ma	Henrici (1998)
Oldest leptodactylid (I) <i>Baurubatrachus pricei</i>	86 Ma	Báez & Perí (1989)
Oldest 'Bufo' (K)	55 Ma (L. Palaeocene)	Báez & Nicoli (2004)
Oldest bufonid (J)	57 Ma (L. Palaeocene)	Báez & Gasparini (1979)
Oldest pelobatid (D) <i>Eopelobates</i>	49 Ma (L. Eocene)	Antunes & Russell (1981)
Oldest ranid (G)	37 Ma (L. Eocene)	Rage (1984)
<i>Bufo</i> : Central–N. American split (L): <i>B. praevis</i>	20 Ma (E. Miocene)	Tihen (1951)
Microhylidae (H) <i>Gastrophryne cf. carolinensis</i>	20 Ma (Hemingfordian, Miocene)	Sanchíz (1998)
<i>Bufo marinus</i> (M)	Mid Miocene (11 Ma)	Sanchíz (1998)

simultaneously estimate phylogeny and divergence times. Fourteen fossil calibrations and three divergence estimates from the literature (presented in Table 3) were used to place priors on the age of nodes within our tree (including the root node). Prior information on clade ages derived from fossil material was implemented as the lower limit of the 95% credibility interval of a normal distribution on the age of the node uniting the descendant clade representative of that fossil and its sister clade. Upper constraints were placed on two of the deeper nodes of our tree (as above) based on generally accepted divergence time of the synapsid–diapsid split (necessarily more recent than the 338 Ma inferred timing of the amniote–amphibian, Ruta *et al.*, 2003), and assuming that the diversification of the extant Anura is more recent than the oldest fossil anuran (*Prosalirus bitis* at 195 Ma; Jenkins & Shubin, 1998; Rocek, 2003). The prior on the age of the root node was based on the generally accepted teleost–tetrapod divergence time of 420 Ma (Ahlberg & Milner, 1994).

While the mitochondrial rRNA data proved useful in analysis of phylogenetic relationships, we did not include sequence data for these loci for the most distant outgroups (*Danio*, *Homo* and *Gallus*) because they were problematic for aligning across divergent taxa and we were thus obligated to exclude these data from

**Table 2** Major data partitions analysed in this study, their characteristics resulting from MP analysis, and the appropriate models used in separate and combined Bayesian and ML data partitions.

the divergence time analyses. For the BEAST analyses we assumed a GTR + I + G model of nucleotide substitution (see above) and an uncorrelated lognormal model of rate variation. The prior for the rate at the root node was set to the median value of the sum of all root-to-tip branch lengths divided by time. The monophyly of some clades strongly supported by phylogenetic analysis was constrained for reasons of computational efficiency and a Yule prior was placed on the branching rates. The results of three independent, 10,000,000-generation analyses were compared and combined in Tracer 1.2 (Rambaut & Drummond, 2003). In order to ascertain the true 'joint prior' of the temporal constraints used in the BEAST analysis, and thus test the strength of signal in our data, we conducted one analysis with only a single ambiguous character in our data matrix.

## RESULTS

### Phylogeny and spatial origin

Our Bayesian phylogeny is relatively robust, with most nodes resulting in  $bp\text{p} > 0.95$  and  $np\text{b} > 70$  (Fig. 1) and is broadly congruent with trees derived from ML and MP methods, as well as

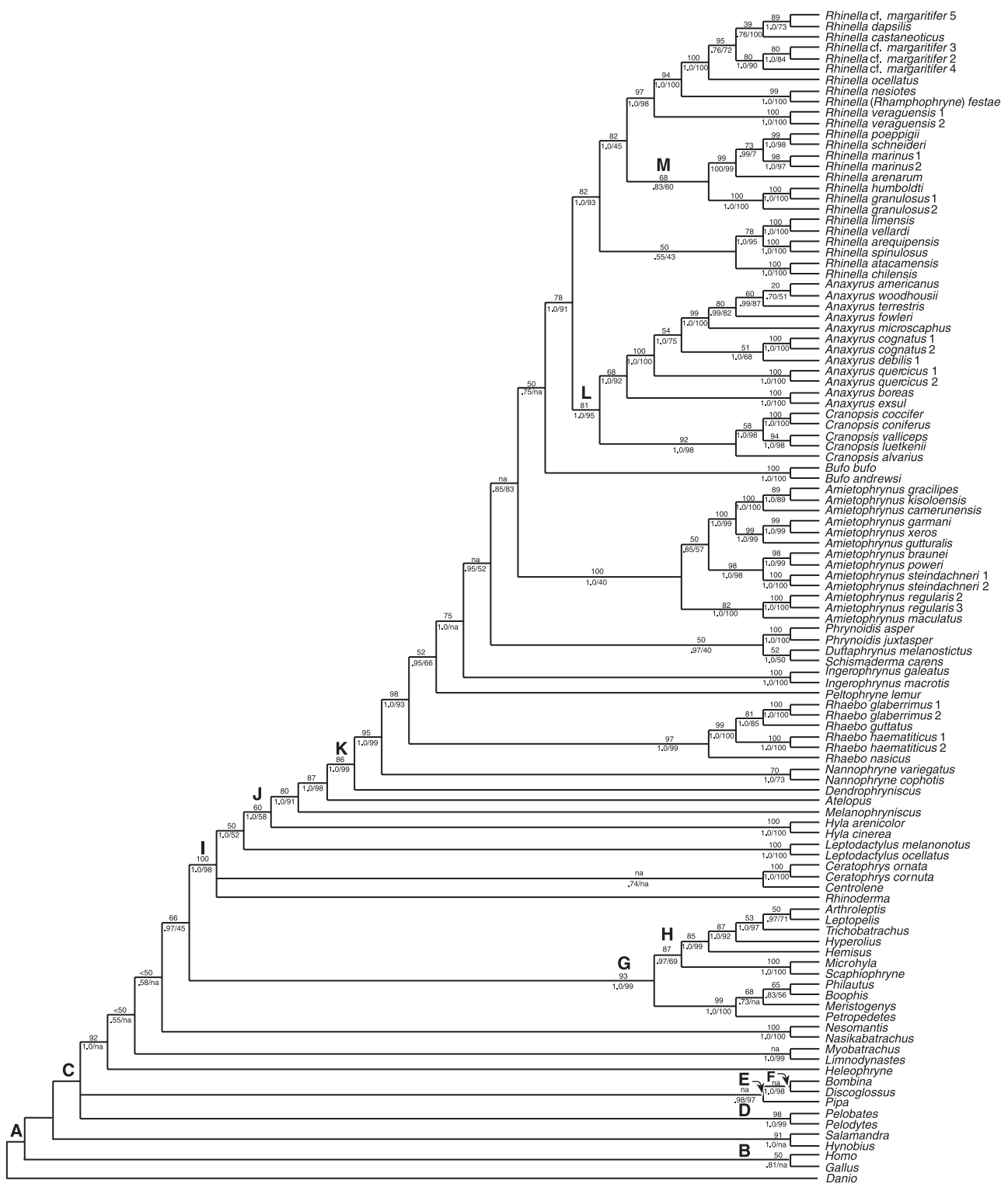


**Figure 1** Bayesian consensus tree resulting from analysis of 3571 bp of combined mitochondrial (*12S*, *tRNA<sup>val</sup>*, *16S* rRNA) and nuclear (*CXCR-4* and *RAG-1*) data. Support values are reported as follows: MP bootstraps above nodes; Bayesian posterior probabilities and ML bootstraps, respectively, below nodes. Lettered nodes (A–M) correspond to fossil calibrations listed in Table 3.

with trees from a prior analysis of mitochondrial, nuclear and morphological data (see Fig. 4 of Pramuk, 2006). However, our topology contrasts with the results of Frost *et al.* (see Fig. 70 of Frost *et al.*, 2006) in several regards (see Discussion).

Generally, conflicts between the topology of Pramuk (2006) and that presented herein (Fig. 1) are in poorly supported nodes. As the phylogenetic relationships of Bufonidae included in this analysis are discussed in depth elsewhere (Pramuk, 2006), and

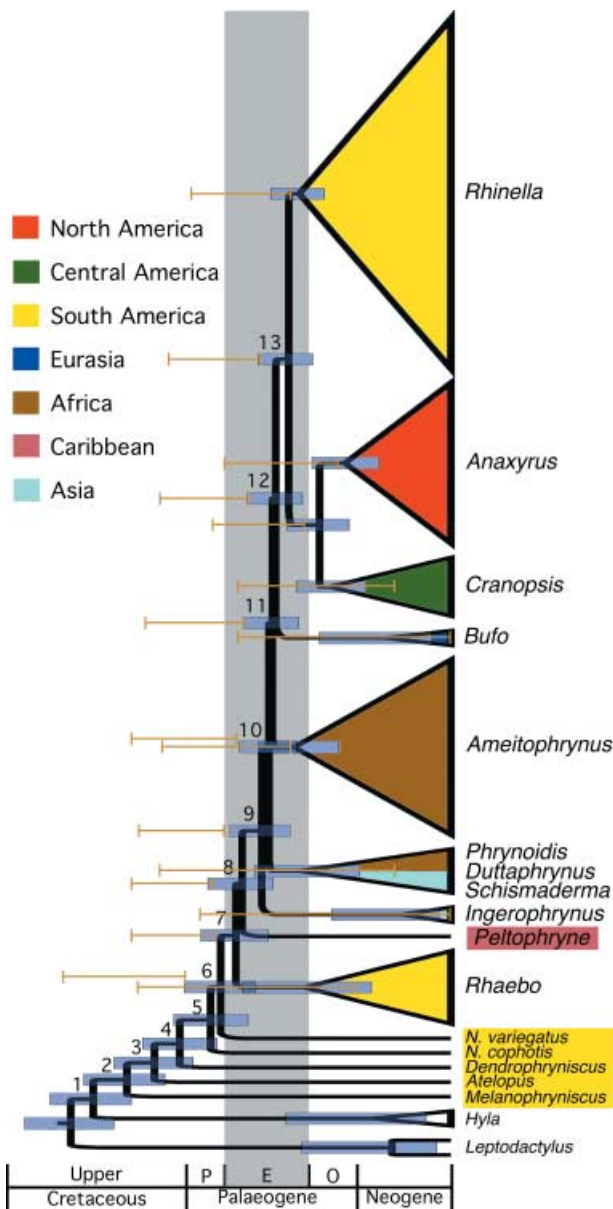


**Figure 2** Bayesian consensus tree reduced from Fig. 1, illustrating divergence time estimates within Bufonidae. Divergence times were estimated from the concatenated data set with a Bayesian method with 13 time constraints from fossil calibrations (fossils are listed in Table 3). Labelled nodes of this tree (1–13) correspond to divergence dates of interest, some of which are discussed in the text. Horizontal bars and shaded rectangles indicate 95% credibility intervals of joint prior and posterior estimate of divergence times, respectively; shading indicates the geographical distribution of each lineage.

because the topologies resulting from these studies are broadly congruent, we do not discuss in detail here the differences between these studies. The vast majority of nodes in our hypothesis (Fig. 1) that are relevant to the understanding of bufonid phylogeny are well supported, providing a reliable phylogenetic framework to assess divergence times. The slight discrepancies resulting from this study and the earlier analysis are likely to result from the slightly different composition of the data sets employed for

both (i.e. in this study: addition of the nuclear marker *CXCR-4*, omission of the nuclear marker *POMC* and morphological data). The *POMC* data were excluded from this study because they were not very informative and were not readily available, unlike the *CXCR-4* and *RAG-1* fragments, for the added Archaeobatrachian and Neobatrachian outgroups.

The topology resulting from this analysis places the older South American clades of Bufonidae as the sister to all remaining true toads (Fig. 1). This topology is consistent with a South American origin for Bufonidae.

### Divergence time estimates and temporal origin

Estimates of divergence times obtained from our analyses suggest that Bufonidae is primarily a post-Gondwanan group [78.3–98.8; 88.2 Ma (95% credibility interval and median, respectively) Fig. 2, node 1], and that clades within it are largely the result of Palaeogene diversification, which agrees with previous estimates of the age of bufonids (e.g. San Mauro *et al.*, 2005). Comparison of posterior estimates of the joint prior indicate that the sequence data are informing the posterior age estimates and that the resulting divergence time estimates are not largely the result of the temporal constraints employed (Fig. 2).

## DISCUSSION

### Temporal origin

Our divergence time estimate for the ancestral node of Bufonidae (78.3–98.8 Ma; node 1; Fig. 2) places the origin of the family in the Upper Cretaceous. Well-constrained geological data (e.g. Pitman *et al.*, 1993; Maisey, 2000) pinpoint the final separation of South America and Africa in the latest Albian of the Early Cretaceous (c. 105 Ma). On the basis of present-day distribution and morphological characters (e.g. Savage, 1973), divergence estimates from immunological distance data (Maxson, 1984), and area cladograms derived from molecular data (Pramuk, 2006), prior investigators have suggested a Gondwanan origin for the true toads. However, an ancient origin for the family has been met with scepticism (Pauly *et al.*, 2004), primarily because of a lack of bufonid fossils that are old enough (none > 60 Ma) to support a pre-Gondwanan origin for the group. Our data fail to support an origin of Bufonidae on Gondwana, as our estimates place the origin of the family after the break-up of South America and Africa (Fig. 3a). Notably, the oldest fossil attributable to the genus formerly known as ‘*Bufo*’ dates from the Late Palaeocene of Itaborai, Brazil (c. 55 Ma; Báez & Nicoli, 2004), with the oldest bufonid being only slightly older (c. 57 Ma; Báez & Gasparini, 1979). The specimen attributed to ‘*Bufo*’ reportedly is of a species aligned with the *Rhinella marinus* group (Báez & Nicoli, 2004). Because this fossil was described on ‘an incomplete basal portion of the left ilium’ (Báez & Nicoli, 2004), it may be reasonable to assume it can only be assigned with confidence to the South American *Rhinella* clade. However, this fossil is considerably older than our posterior estimate for *Rhinella* (node 13, Fig. 2; 31–44 Ma). Complicating matters, the Bufonidae are notoriously

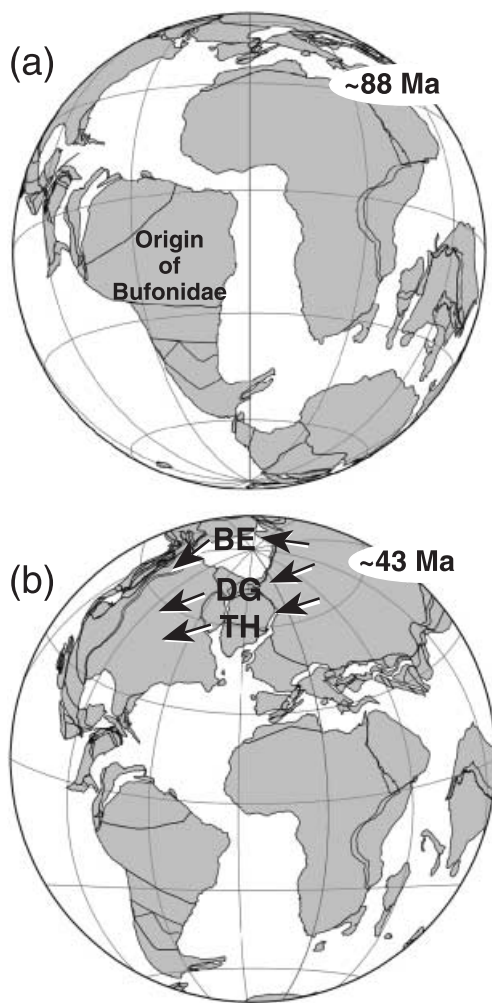


**Figure 3** Maps illustrating two key geological intervals relevant to bufonid biogeography. (a) The Earth at c. 88 Ma, illustrating the origin of Bufonidae, which according to our data occurred at 88 Ma (point estimate; 78–99 Ma credibility interval) after the break-up of Gondwana c. 105 Ma (Reyment & Dingle, 1987; Pitman *et al.*, 1993; Maisey, 2000). Although our data do not clarify how ancestral bufonids may have dispersed from South America back into the Old World, giving rise to African and Eurasian clades, our data suggest they may have expanded northward into Central and North America and subsequently into Eurasia via Beringia. (b) Proposed migration of bufonids from Eurasia back into North America during the Eocene. Three routes from Eurasia are possible including the Beringian (BE), De Geer (DG) and Thulean (TH) land bridges. The high latitude ( $> 70^\circ$  N) during the Eocene of BE and DG relative to TH makes the latter route more probable for an ectothermic lineage. Our median estimate for the divergence of Old and New World bufonids is 43 Ma, a date that corresponds to the Eocene thermal maxima, when ectothermic lineages were likely to have migrated at higher latitudes via Beringia or trans-Atlantic land bridges (map modified from Fig. 8 of Irving, 2005). Our data indicate that climatic fluctuations of the Eocene played a significant role in shaping the current distribution of true toads. Maps were generated from the Ocean Drilling Stratigraphic Network (ODSN) website <http://www.odsn.de/odsn/services/paleomap/paleomap.html>. Note: continental outlines indicate hypothetical plate margins rather than shorelines (the limits of the latter being particularly contentious).

morphologically conserved (Pramuk, 2006). Thus, this may be yet another instance of the conservative variation in morphology confounding the taxonomic assignment of material – a situation we would expect to be particularly problematic in assigning fragmentary fossil remains. It is worth noting that a similar problem has plagued cichlid fish biogeography for decades, as their apparent Gondwanan distribution was confounded by the fact that the oldest fossil material of this group was from the Eocene (c. 38–54 Ma; Chakrabarty, 2004). Recent investigations (e.g. Chakrabarty, 2004; but see Vences *et al.*, 2001) have provided strong support for a Gondwanan origin of the Cichlidae and have highlighted the paucity of the fossil record from this time and the perils of inferring true absence.

Also confounding the hypothesis of a Gondwanan distribution is the absence of extant or fossil bufonids from Madagascar and Australia–New Guinea. Biological continuity of these land masses with South America via Antarctica into the Late Cretaceous (Madagascar) and Palaeogene (Australia) is well supported by both geological and biological data (e.g. Sampson *et al.*, 1998; Hay *et al.*, 1999; Noonan & Chippindale, 2006). However, this apparently enigmatic absence is not unique to bufonids. Other groups with a wide or ‘Gondwanan distribution’, such as boine snakes, iguanine lizards, pelomedusoid turtles, abelisauroid theropod dinosaurs, cichlid fish and gondwanatherian mammals, are also notably absent from Australia (Sampson *et al.*, 1998; Vences *et al.*, 2001; Noonan & Chippindale, 2006). That so many groups of Gondwanan age are absent from this continent argues for a barrier to dispersal on Antarctica (Janis, 1993). The absence from Madagascar is less common in Gondwanan groups, though these are taxa (e.g. reptiles, birds and mammals) that are likely to have a greater tolerance than anurans to climatic fluctuations and salinity that may have been encountered along this terrestrial connection. The absence of bufonids from Madagascar may also be explained simply as an effect of time. All of the aforementioned Gondwanan groups present on this island are either extinct or persist at very low levels of diversity (one to three species).

### Spatial origin

One of the most striking aspects of this (Fig. 1) and other recent analyses of bufonid phylogeny (Pauly *et al.*, 2004; Frost *et al.*, 2006; Pramuk, 2006) is the paraphyly of the South American bufonids (now comprising the ‘older’ *Atelopus*, *Melanophryniscus*, *Rhaebo*, *Nannophryne* and the relatively ‘recent’ *Rhinella*). Given this surprising pattern of relationships and the inferred origin of the group in South America (see above), the origin of the South American *Rhinella* and their sister group (the North and Central American clade comprising *Anaxyrus* and *Cranopsis*), suggests a secondary invasion of the New World.

The post-Gondwanan age and phylogenetic placement of Old World bufonids suggests an out-of-South America dispersal in the early Palaeogene. The low tolerance of bufonids to salinity makes overwater dispersal of bufonids from South America to Africa or Eurasia unlikely, but not impossible, as long-distance saltwater dispersal has been invoked to explain the distribution

of other Neobatrachian frogs (see de Queiroz, 2005, for a review). The only plausible overland route for this group would be a northward expansion into Central America, North America and then Eurasia via Beringia. This is similar to the hypothesis proposed by Blair (1972) (see also Fig. 1 of Pauly *et al.*, 2004). Despite our relatively poor sampling of Asian bufonids, our recovered phylogenetic pattern, combined with presumed terrestrial connections (Beringia, Thulean and De Geer land bridges), leads us to favour the Beringian connection over those of the North Atlantic for this migration.

Our posterior estimates of divergence times suggest that the New World clade comprising *Rhinella*, *Cranopsis* and *Anaxyrus* diverged from its Old World relatives in the Eocene (43.3 Ma, 36.5–50 Ma; median and credibility interval, respectively). There are three putative land bridges that joined Eurasia with North America at different times throughout the Cenozoic, including the Beringia, Thulean and De Geer land bridges (Fig. 3b). Here we investigate these three possible routes given our data and known geological evidence. While some authors have favoured an Asiatic origin for Nearctic–Palaeartic dispersal (e.g. Blair, 1972), frequently without consideration of documented alternative routes (Macey *et al.*, 2006), the close relationships of the ‘recent’ New World clade with the exclusively Eurasian + African clades suggests the possibility a trans-Atlantic route. In addition, although Bufonidae could have migrated via Beringia during the Eocene, the high latitude of this route (69–75° N; Tiffney, 1985) probably prohibited its use by ectothermic taxa for most of this time (Davis *et al.*, 2002). During the Eocene, dispersal of bufonids from the Old World to the New World would have been facilitated by a boreotropical connection, or ‘North American land bridge’ via a series of connections including the Thulean and De Geer land bridges across the North Atlantic (Tiffney, 1985; Davis *et al.*, 2002; Fig. 3b). This pattern of European/North American, Palaeogene faunal similarity with an apparent disruption in the Eocene has been documented in numerous plant (Tiffney, 1985; Davis *et al.*, 2002) and animal (e.g. Dawson *et al.*, 1976; Estes & Hutchison, 1980; Dawson, 2001) groups.

We suggest, based on our divergence time estimates, that secondary dispersal of Bufonidae to the New World most likely occurred during the latest Palaeocene thermal maximum (LPTM), which occurred in the early Cenozoic (65–40 Ma) and reached its peak 55 Ma (lasting for c. 100–140 kyr (e.g. Peters & Sloan, 2000; Thomas, 2004) via the Thulean (Iceland–Faeroes) land bridge (situated below 62° N), which was significantly lower in latitude than the Beringia or the De Geer land connections (c. 74° N) and therefore more amenable to dispersal by ectothermic animals. An analysis of the  $\delta^{13}\text{C}$  record at the latest Palaeocene thermal maximum (Peters & Sloan, 2000) suggests that of the three land bridges, only the Thulean and Beringian routes are likely to have maintained year-round temperatures above freezing, though fossil evidence suggests the De Geer route was suitable for ectotherms (turtles; Dawson *et al.*, 1976; Estes & Hutchison, 1980). It has been suggested that both the Thulean and De Geer routes became interrupted in the early Eocene (Peters & Sloan, 2000; Sanmartín *et al.*, 2001), a timing that closely fits our findings.

Vertebrate palaeontological data indicate that the faunas of North America and Europe during the early Eocene were broadly overlapping. This similarity peaked in the early Eocene when approximately 60% of known European genera were shared with North America (Tiffney, 1985; Sanmartín *et al.*, 2001). A detailed study of Nearctic patterns of relationship by Sanmartín *et al.* (2001) revealed that though Beringian dispersal appears to have occurred more frequently than trans-Atlantic dispersal, the difference is insignificant. Furthermore, the findings of Sanmartín *et al.* (2001) indicate that the height of Beringian dispersal occurred in pre-Cretaceous and Quaternary times whereas trans-Atlantic dispersal peaked in the Palaeogene, again consistent with our Eocene estimate of the timing divergence between Eurasian and New World bufonids. Due to the very broad temporal scale of the inferred terrestrial connection between the eastern Palaeartic and the western Nearctic (via Beringia; see Fig. 10 of Sanmartín *et al.*, 2001) that entirely overlaps the timing of a trans-Atlantic connection, divergence times alone cannot support one hypothesis in favour of the other. Such differentiation will rely on the temporal overlap of divergence times with the comparatively narrow window of a trans-Atlantic terrestrial connection and phylogenetic patterns, suggesting a close European/North American relationship.

#### North America + Central America–South America split

The sister group relationship and reciprocal monophyly of the South American *Rhinella* and the North (*Anaxyrus*) + Central (*Cranopsis*) American clades recovered here is consistent with the results of prior analyses of bufonids (e.g. Pramuk, 2006); here, the estimated split of these clades is 41 Ma and 34–47 Ma (median and credibility interval, respectively). The differentiation between the South and North + Central American groups appears to have followed shortly after the arrival of bufonids in the Americas with diversification within each clade beginning almost immediately. This pattern suggests that the initial invasion of the Americas was rapid and occurred at a time when there was little hindrance to southward dispersal from North America. Southward dispersal of ectothermic groups of organisms (e.g. bufonids) may have been facilitated by cooler global temperatures following the Eocene (Irving, 2005) and intermittent terrestrial connections (see Figs 3 & 5 of Sanmartín *et al.*, 2001). Southward dispersal of North American taxa at this time has been suggested for other groups as well (e.g. the plant *Styrax*; Fritsch, 1999). Isolation of North America from South America (and potentially a Middle American isolate) from the Neogene until c. 3 Ma (see Fig. 5 of Sanmartín *et al.*, 2001) suggests a mechanism for the diversification of these three geographical lineages.

#### Caribbean lineage

Our Bayesian estimates for the West Indian clade allow us to test dispersalist versus vicariant hypotheses for *Peltophryne*, a subject that has been explored extensively (e.g. Pramuk, 2002; Frost *et al.*, 2006). Our estimate for the age of this clade is 51 Ma (44–60 Ma), thus precluding the possibility of this taxon representing a Cretaceous



Caribbean lineage that survived the K/T impact event (65 Ma). Regardless, our estimate for the West Indian toads confirms earlier suggestions (e.g. Frost *et al.*, 2006; Pramuk, 2006) that this represents a comparatively ancient clade within Bufonidae.

Existing models of Caribbean biogeography are challenged by the complex and controversial geological history of the Caribbean (e.g. Iturralde-Vincent & MacPhee, 1999). Although the timing of island formation and divergence is not agreed upon, a recent estimate for the age of the modern-day Greater Antilles places them at no older than middle Eocene (Iturralde-Vincent & MacPhee, 1999), indicating that the present day islands are younger than our 51 Ma Palaeocene–early Eocene estimate for *Peltophryne*. Interestingly, age estimates for other groups of West Indian taxa are remarkably close to our estimates for the native Caribbean toads. For example, the clade leading to the endemic Cuban night lizard *Cricosaura* was estimated to be 54 Ma (43–64.9 Ma; Vicario *et al.*, 2003) and the split between Middle American cichlids and Greater Antillean species is estimated to be 47 Ma (42–52 Ma; Chakrabarty, 2006). Although a different method (penalized likelihood) and different genes were used to estimate the divergence dates of *Cricosaura* and the West Indian cichlids, the similarity in divergence estimates for these unrelated Caribbean clades is intriguing.

### Phylogeny

Some aspects of our phylogeny differ markedly from those of the studies of Frost *et al.* (2006) and Pauly *et al.* (2004). These authors recovered *Bufo margaritifera* (*Rhinella* *vide* Frost *et al.*, 2006) and *Rhamphophryne festae* as sister to bufonids from Asia including *Bufo* (= *Ingerophrynus* *vide* Frost *et al.*, 2006) *galeatus* and *Bufo divergens*. In our analyses, *Rhinella margaritifera* and *Rhamphophryne* are sister groups and are nested within the large clade of South American *Bufo* (= *Chaunus*, *vide* Frost *et al.*, 2006). These two taxa in the analysis of Frost *et al.* (2006) were represented by a relatively small subset of data (an average of 1342 bp of 12S and 16S data) resulting from an unpublished thesis (Gluesenkamp, 2001). We suspect that the phylogenetic placement recovered by Frost *et al.* (2006) is an artefact of poor taxon and character sampling within the *Rhinella* and *Rhamphophryne* clades. Frost *et al.* (2006) state ‘[if] *Rhinella* Fitzinger, 1828, [is] found to be nested within *Chaunus* Wagler, 1828, the name *Rhinella* will take precedence for the inclusive group’. In accordance with these authors we reassign *Chaunus* to *Rhinella*.

Another striking difference in this study compared with results of prior analyses is the well-supported placement of the North American clade (*Anaxyrus*) as sister to Central American taxa (*Cranopsis*). In contrast, the other analyses supported a [North America (South + Central America)] relationship (Pauly *et al.*, 2004; Frost *et al.*, 2006).

### General conclusions

Despite numerous investigations into the evolutionary history of Bufonidae, ours is the first to employ newly developed Bayesian methods to estimate divergence times for this widespread family.

Our study illustrates the utility of increasing outgroup sampling of groups with a relatively detailed fossil record to provide calibration points outside of a fossil-poor clade of interest. Our findings reveal a surprisingly recent age for the origin of the nearly cosmopolitan Bufonidae (78–98 Ma). The relatively rapid spread of this group across the globe in the Cenozoic, accompanied by regional diversification is truly remarkable – particularly so given that the earliest occurrence of any lineage outside South America is no earlier than 52 Ma (node 9, Fig. 2; 38–52 Ma). Subsequent to their dispersal out of South America, the entire radiation of the major lineages (genera) of extant bufonid frogs took place in the Eocene. Tracking the terrestrial route for this global dispersal is likely to remain unresolved due to the temporal overlap of alternative routes. Although a Beringian route has, of late, served as the preferred route for biogeographers examining patterns of biotic exchange between the Nearctic and Palaearctic, the existence of a North Atlantic connection, and its suitability for temperate/tropical taxa, is argued here and must be considered in studies of Laurasian biogeography. What is clear is that the climatic fluctuations of the Eocene, recorded in so many other biotic and geological elements, played a significant role in shaping the current distribution of this group of amphibians.

### ACKNOWLEDGEMENTS

This material is based upon work supported by the National Science Foundation under awards DEB 0132227 [‘The phylogeny of the Xantusiidae, and its placement within the Scleroglossa (Reptilia; Squamata)’] and EF 0334966 (‘Assembling the tree of life – the deep scaly project: resolving higher level squamate phylogeny using genomic and morphological approaches’).

### REFERENCES

- Ahlberg, P.E. & Milner, A.R. (1994) The origin and early diversification of the tetrapods. *Nature*, **368**, 507–514.
- Alfaro, M.E., Zoller, S. & Lutzoni, F. (2003) Bayes or bootstrap? A simulation study comparing the performance of Bayesian Markov chain Monte Carlo sampling and bootstrapping in assessing phylogenetic confidence. *Molecular Biology and Evolution*, **20**, 255–266.
- Antunes, M.T. & Russell, D.E. (1981) Le gisement de Silveirinha (Bas Mondego, Portugal): la plus ancienne faune de vertébrés éocènes connue en Europe. *Comptes Rendus de l’Académie des Sciences de Paris, Série II*, **293**, 1099–1102.
- Báez, A.M. & Gasparini, Z.B. (1979) The South American herpetofauna: an evaluation of the fossil record. *The South American herpetofauna: its origin, evolution and dispersal* (ed. by W.E. Duellman), Museum of Natural History, University of Kansas Monograph No. 7, pp. 29–55.
- Báez, A.M. & Nicoli, L. (2004) Bufonid toads from the Late Oligocene beds of Salla Bolivia. *Journal of Vertebrate Paleontology*, **24**, 73–79.
- Báez, A.M., & Perí, S. (1989) *Baurubatrachus pricei*, nov. gen. et sp., un Anuro del Cretacio Superior de Minas Gerais, Brasil. *Anais Academica Brasileira Ciencias*, **61**, 447–458.

- Benton, M.J. (1997) *Vertebrate paleontology*, 2nd edn. Chapman & Hall, London.
- Biju, S.D. & Bossuyt, R. (2003) New frog family from India reveals an ancient biogeographical link with the Seychelles. *Nature*, **425**, 711–714.
- Blair, W.F. (1972) Summary. *Evolution in the genus Bufo* (ed. by W.F. Blair), pp. 329–343. University of Texas Press, Austin, TX.
- Castresana, J. (2000) Selection of conserved blocks from multiple alignments for their use in phylogenetic analysis. *Molecular Biology and Evolution*, **17**, 540–552.
- Chakrabarty, P. (2004) Cichlid biogeography: comment and review. *Fish and Fisheries*, **5**, 97–119.
- Chakrabarty, P. (2006) Systematics and historical biogeography of Greater Antillean Cichlidae. *Molecular Phylogeny and Evolution*, **39**, 619–627.
- Chiari, Y.K., Vences, M., Vietes, D.R., Rabemananjara, F., Bora, P., Ramilijaona, Ravoahangimalala, O. & Meyer, A. (2004) New evidence for parallel evolution of colour patterns in Malagasy poison frogs (*Mantella*). *Molecular Ecology*, **13**, 37–63.
- Davis, C.C., Bell, C.D., Mathews, S. & Donoghue, M.J. (2002) Laurasian migration explains Gondwanan disjunctions: Evidence from Malpighiaceae. *Proceedings of the National Academy of Sciences USA*, **99**, 6833–6837.
- Dawson, M.R. (2001) Early Eocene rodents (Mammalia) from the Eureka Sound group of Ellesmere Island, Canada. *Canadian Journal of Earth Science*, **38**, 1107–1116.
- Dawson, M.R., West, R.M., Langston, W., Jr. & Hutchison, J.H. (1976) Paleogene terrestrial vertebrates: northernmost occurrence, Ellesmere Island, Canada. *Science*, **192**, 781–782.
- de Queiroz, A. (2005) The resurrection of oceanic dispersal in historical biogeography. *Trends in Ecology & Evolution*, **20**, 68–73.
- De Rijk, P.Y., Van de Peer, Y., Chapelle, S. & De Wachter, R. (1994) Database on the structure of large ribosomal subunit DNA. *Nucleic Acids Research*, **22**, 3495–3501.
- Drummond, A.J., Ho, S.Y.W., Phillips, M.J. & Rambaut, A. (2006) Relaxed phylogenetics and dating with confidence. *PLoS Biology*, **4**, e88.
- Drummond, A.J. & Rambaut, A. (2003) BEAST, version 1.0. (BEAST Website [http://beast.bio.ed.ac.uk/Main\\_Page](http://beast.bio.ed.ac.uk/Main_Page).)
- Estes, R. & Hutchison, J.H. (1980) Eocene lower vertebrates from Ellesmere Island, Canadian Arctic Archipelago. *Palaeogeography, Palaeoclimatology, Palaeoecology*, **30**, 325–347.
- Evans, S.E., Milner, A.R. & Musset, F. (1990) A discoglossid frog from the Middle Jurassic of England. *Palaeontology*, **33**, 299–311.
- Felsenstein, J. (1985) Confidence limits on phylogenies: an approach using the bootstrap. *Evolution*, **39**, 783–791.
- Fritsch, P.W. (1999) Phylogeny of *Styrax* based on morphological characters, with implications for biogeography and infrageneric classification. *Systematic Botany*, **24**, 356–378.
- Frost, D.R., Grant, T., Faivovich, J., Bain, R.H., Haas, A., Haddad, C.F.B., de Sá, R.O., Channing, A., Wilkinson, M., Donnellan, S.C., Raxworthy, C.J., Campbell, J.A., Blotto, B.L., Moler, P., Drewes, R.C., Nussbaum, R.A., Lynch, J.D., Green, D.M. & Wheeler, W.C. (2006) The amphibian tree of life. *Bulletin of the American Museum of Natural History*, no. 297.
- Gluesenkamp, A.G. (2001) *Developmental mode and adult morphology in bufonid frogs: a comparative analysis of correlated traits*. PhD Dissertation, The University of Texas at Austin.
- Goebel, A.M., Donnelly, J.M. & Atz, M.E. (1999) PCR primers and amplification methods for 12S ribosomal DNA, the control region, cytochrome oxidase I, and cytochrome *b* in bufonids and other frogs, and an overview of PCR primers which have amplified DNA in amphibians successfully. *Molecular Phylogenetics and Evolution*, **11**, 163–199.
- Graybeal, A. (1997) Phylogenetic relationships of bufonid frogs and tests of alternate macroevolutionary hypotheses characterizing their radiation. *Zoological Journal of the Linnean Society*, **119**, 297–338.
- Hay, W.W., DeConto, R.M., Wold, C.N., Wilson, K.M., Voigt, S., Schulz, M., Wold, A.R., Dullo, W., Ronov, A.B., Balukhovskiy, A.N. & Söding, E. (1999) Alternative global Cretaceous paleogeography. *Evolution of the Cretaceous ocean–climate system* (ed. by E. Barrera and C. Johnson), Geological Society of America Special Paper 332, pp. 1–47. Geological Society of America, Boulder, CO.
- Henrici, A.C. (1998) A new pipoid anuran from the Late Jurassic Morrison Formation at Dinosaur National Monument, Utah. *Journal of Vertebrate Paleontology*, **18**, 321–332.
- Hillis, D.M. & Bull, J.J. (1993) An empirical test of bootstrapping as a method for assessing confidence in phylogenetic analysis. *Systematic Biology*, **42**, 182–192.
- Irving, E. (2005) The role of latitude in mobilism debates. *Proceedings of the National Academy of Sciences USA*, **102**, 1821–1828.
- Iturralde-Vincent, M.A. & MacPhee, R.D.E. (1999) Paleogeography of the Caribbean region: implications for Cenozoic biogeography. *Bulletin of the American Museum of Natural History*, no. 238, 1–95.
- Janis, C.M. (1993) Tertiary mammal evolution in the context of changing climates, vegetation, and tectonic events. *Annual Review of Ecology and Systematics*, **24**, 467–500.
- Jenkins, F.A., Jr & Shubin, N. (1998) *Prosalirus bitis* and the anuran caudopelvic mechanism. *Journal of Vertebrate Paleontology*, **18**, 495–510.
- Macey, J.R., Schulte, J.A. II, Strasburg, J.L., Brisson, J.A., Larson, A., Ananjeva, N.B., Wang, Y., Parham, J.F. & Papenfuss, T.J. (2006) Assembly of the eastern North American herpetofauna: new evidence from lizards and frogs. *Biology Letters*, **2**, 388–392.
- Maisey, J.G. (2000) Tectonics, the Santana Lagerstätten, and the implications for late Gondwanan biogeography. *Biological relationships between Africa and South America* (ed. by P. Goldblatt), pp. 435–454. Yale University Press, New Haven, CT.
- Maxson, L.R. (1984) Molecular probes of phylogeny and biogeography in toads of the widespread genus *Bufo*. *Molecular Biology and Evolution*, **1**, 324–356.
- Noonan, B.P. & Chippindale, P.T. (2006) Vicariant origin of Malagasy reptiles supports Late Cretaceous Antarctic landbridge. *The American Naturalist*, **168**, 730–741.

- Pauly, G.B., Hillis, D.M. & Cannatella, D.C. (2004) The history of a Nearctic colonization: Molecular phylogenetics and biogeography of the Nearctic toads (*Bufo*). *Evolution*, **58**, 2517–2535.
- Pennington, T.R. (1996) Molecular and morphological data provide phylogenetic resolution at different hierarchical levels in *Andira*. *Systematic Biology*, **45**, 496–515.
- Peters, R.B. & Sloan, L.C. (2000). High concentrations of greenhouse gases and polar stratospheric clouds: a possible solution to high-latitude faunal migration at the latest Paleocene thermal maximum. *Geology*, **28**, 979–982.
- Pitman W.C., Cande S., LaBrecque J. & Pindell J. (1993) Fragmentation of Gondwana: the separation of Africa from South America. *Biological relationships between Africa and South America* (ed. by P. Goldblatt), pp. 15–34. Yale University Press, New Haven, CT.
- Posada, D. & Crandall, K.A. (1998) Modeltest: Testing the model of DNA substitution. *Bioinformatics*, **14**, 817–818.
- Pramuk, J.B. (2002) Morphological characters and cladistic relationships of West Indian toads (Anura: Bufonidae). *Herpetological Monographs*, **16**, 121–151.
- Pramuk, J.B. (2006) Phylogeny of South American *Bufo* (Anura: Bufonidae) inferred from combined evidence. *Zoological Journal of the Linnean Society*, **146**, 407–452.
- Rage, J.C. (1984) Are the Ranidae (Anura, Amphibia) known prior to the Oligocene? *Amphibia-Reptilia*, **5**, 281–288.
- Rambaut, A. & Drummond, A. (2003) *Tracer*, version 1.2. (Available from <http://evolve.zoo.ox.ac.uk/software.html?id=tracer>.)
- Roček, Z. (2003) Mesozoic anurans. *Amphibian biology. Volume 4. Palaeontology* (ed. by H. Heatwole), pp. 1295–1331. Surrey Beatty & Sons, Chipping Norton, NSW.
- Ronquist, F. & Huelsenbeck, J.P. (2003) MrBayes 3: Bayesian phylogenetic inference under mixed models. *Bioinformatics*, **19**, 1572–1574.
- Ruta, M., Coates, M. I. & Quicke, D.L. (2003) Early tetrapod relationships revisited. *Biological Review*, **78**, 241–345.
- Sampson, S.D., Witmer, L.M., Forster, C.A., Krause, D.W., O'Connor, P.M., Dodson, P. & Ravoavy, F. (1998) Predatory dinosaur remains from Madagascar: implications for the Cretaceous biogeography of Gondwana. *Science*, **280**, 1048–1051.
- Sanchíz, B. (1998) Salientia. *Handbuch der Paläoherpetologie* (ed. by P. Wellnhofer), Part 4, pp. 1–275. Verlag Dr. Friedrich Pfeil, Munich.
- Sanmartín, I., Enghoff, H. & Ronquist, F. (2001) Patterns of animal dispersal, vicariance and diversification in the Holarctic. *Biological Journal of the Linnean Society*, **73**, 345–390.
- San Mauro, D., Vences, M., Alcobendas, M., Zardoya, R. & Meyer, A. (2005) Initial diversification of living amphibians predated the breakup of Pangaea. *The American Naturalist*, **165**, 590–599.
- Savage, J.M. (1973) The geographic distribution of frogs: patterns and predictions. *Evolutionary biology of the anurans: contemporary research on major problems* (ed. by J. Vial), pp. 351–446. University of Missouri Press, Columbia, MO.
- Swofford, D.L. (2002) *Phylogenetic analysis using parsimony (PAUP)*, version 4.0b10. Computer program distributed by the Illinois Natural History Survey, Champaign, IL.
- Thomas, D.J. (2004) Evidence for production of North Pacific deep waters during the early Cenozoic greenhouse. *Nature*, **430**, 65–68.
- Thompson, J.D., Gibson, T.J., Plewniak, F., Jeanmougin, F. & Higgins, D. (1997) The ClustalX Windows interface: flexible strategies for multiple sequence alignment aided by quality analysis tools. *Nucleic Acids Research*, **25**, 4876–4882.
- Thorne, J.L. & Kishino, H. (2002) Divergence time and evolutionary rate estimation with multilocus data. *Systematic Biology*, **51**, 689–702.
- Thorne, J.L., Kishino, H. & Painter, I.S. (1998) Estimating the rate of evolution of the rate of molecular evolution. *Molecular Biology and Evolution*, **15**, 1647–1657.
- Tiffney, B.H. (1985) Perspectives on the origin of the floristic similarity between eastern Asia and eastern North America. *Journal of the Arnold Arboretum*, **66**, 73–94.
- Tihen, J.A. (1962) Anuran remains from the Miocene of Florida, with the description of a new species of *Bufo*. *Copeia*, **1951**, 230–235.
- Tihen, J.A. (1965) A review of New World fossil bufonids. *American Midland Naturalist*, **68**, 1–50.
- Van de Peer, Y., Van den Broeck, I., De Rijk, P. & De Wachter, R. (1994) Database on the structure of small subunit RNA. *Nucleic Acids Research*, **22**, 3488–3494.
- Vences, M., Freyhof, J., Sonnenberg, R., Kosuch, J. & Veith, M. (2001) Reconciling fossils and molecules: Cenozoic divergence of cichlid fishes and the biogeography of Madagascar. *Journal of Biogeography*, **28**, 1091–1099.
- Vicario, S., Caccone, A. & Gauthier, J. (2003) Xantusiid ‘night’ lizards: a puzzling phylogenetic problem revisited using likelihood-based Bayesian methods on mtDNA sequences. *Molecular Phylogenetics and Evolution*, **26**, 243–261.

## BIOSKETCHES

**Jennifer Pramuk** and **Brice Noonan** performed this research at Brigham Young University (BYU) where they had appointments as postdoctoral research associates in the laboratory of Jack W. Sites, Jr. Brice Noonan is now a post-doctoral associate at Duke University and Jennifer Pramuk is the Curator of Herpetology at the Bronx Zoo/Wildlife Conservation Society.

**Jack W. Sites, Jr** is a Professor of Integrative Biology at Brigham Young University. A portion of this research included mentorship of **Tasia Robertson**, who gained field and laboratory experiences while working on this project and graduated with a degree in biology from BYU in spring of 2006.

Editor: Brad Murray

## SUPPLEMENTARY MATERIAL

The following supplementary material is available for this article:

**Appendix S1** Outgroup and ingroup taxa included in this analysis.

This material is available as part of the online article from:

<http://www.blackwell-synergy.com/doi/abs/10.1111/j.1466-8238.2007.00348.x>

(This link will take you to the article abstract).

Please note: Blackwell Publishing is not responsible for the content or functionality of any supplementary materials supplied by the authors. Any queries (other than missing material) should be directed to the corresponding author for the article.

1           **Appendix S1** Outgroup and ingroup taxa included in this analysis. Most outgroup taxa are from Biju  
 2 & Bossuyt (2003). Other specimens include GenBank numbers, collection numbers, and locality data for  
 3 individuals sequenced for 12S, tRNA<sup>val</sup>, 16S and RAG-1 for a prior study (Pramuk, 2006). In addition,  
 4 GenBank numbers are presented for CXCR-4 sequenced for this study.

5

Outgroup Genera (from Biju and Bossuyt [7]):	Species from Genbank	12S,16S	RAG-1	CXCR-4
Alytidae	<i>Discoglossus pictus auritus</i>	AY364342, AY364364	AY364202	AY364172
Arthroleptidae	<i>Arthroleptis variabilis</i>	AY364347, AY322301	AY364210	AY364180
Astylosternidae	<i>Trichobatrachus robustus</i>	AY322304, AY322274	AY364212	AY364182
Arthroleptidae	<i>Leptopelis kivuensis</i>	AY322328, AY322275	AY364211	AY364181
Bombinatoridae	<i>Bombina orientalis</i>	AY364346, AY364368	AY364207	AY364177
Bufo	<i>Bufo melanostictus</i>	AF249001, AF249061	AY364197	AY364167
Centrolenidae	<i>Centrolene prosoblepon</i>	AY364358, AY364379	AY364223	AY364193
Ceratophrynidae	<i>Ceratophrys ornata</i>	AY364353, AY364374	AY364218	AY364188
Cycloramphidae	<i>Rhinoderma darwinii</i>	AY364357, AY364378	AY364222	AY364192
Heleophrynidae	<i>Heleophryne purcelli</i>	AY364356, AY364377	AY364221	AY364191
Hemisotidae	<i>Hemisis marmoratus</i>	AY364351, AY364372	AY364216	AY364186
Hylidae	<i>Hyla arenicolor</i>	AY364355, AY364376	AY364220	AY364190
Hyperoliidae	<i>Hyperolius</i> sp.	AF249002, AF249033	AY364208	AY364178
Leptodactylidae	<i>Leptodactylus melanonotus</i>	AY364359, AY364380	AY364224	AY364194
Limnodynastidae	<i>Limnodynastes salmini</i>	AY364354, AY364375	AY364219	AY364189
Mantellidae	<i>Boophis xerophilus</i>	AF249008, AF249038	AY364209	AY364179
Microhylidae	<i>Microhyla ornata</i>	AF249003, AF249060	AY364198	AY364168
Myobatrachidae	<i>Myobatrachus gouldii</i>	AY364361, AY364382	AY364226	AY364196
Pelobatidae	<i>Pelobates cultripes</i>	AY364341, AY364363	AY364201	AY364171
Pelodytidae	<i>Pelodytes punctatus</i>	AY364343, AY364365	AY364203	AY364173
Petropedetidae	<i>Petropedetes</i> cf. <i>parkeri</i>	AY364348, AY364369	AY364213	AY364183

**Additional outgroup taxa sequenced for this study:**

	<b>ID Number; Locality</b>	<b>12S, tRNA<sup>val</sup>, 16S</b>	<b>RAG-1</b>	<b>CXCR-4</b>
Pipidae	<i>Pipa pipa</i>	AY364344, AY364366	AY364204	AY364174
Ranidae	<i>Meristogenys kinabaluensis</i>	AY322317, AY322292	AY364206	AY364176
Rhacophoridae	<i>Philautes wynaadensis</i>	AF249031, AF249059	AY364199	AY364169
Scaphiophryinae	<i>Scaphiophryne marmorata</i>	AY364345, AY364367	AY364205	AY364175
Sooglossidae	<i>Nasikabatrachus sahyadrensis</i>	AY364360, AY364381	AY364225	AY364195
Sooglossidae	<i>Nesomantis thomasseti</i>	AY364352, AY364373	AY364217	AY364187
<i>Atelopus peruensis</i>	KU 211632; Peru: Cajamarca, Cajamarca Abra Quilsh.	DQ158419	DQ158345	DQ306495
<i>Ceratophrys cornuta</i>	KU 215537; Peru: Madre de Dios, Cuzco Amazonico.	AY326014	AY364218	DQ306491
<i>Dendrophryniscus</i> sp.	QCAZ 883; Ecuador.	DQ158420	DQ158346	DQ306496
<i>Eleutherodactylus w-nigrum</i>	KU 218136; Ecuador, Bolivar, 29 km E Guaranda on road to Riobamba.	AY326004	DQ158344	--
<i>Hyla cinerea</i>	KU 207358; USA: Mississippi, Bluff Lake, Noxubee National Wildlife Refuge.	AY680271	DQ158342	DQ306493
<i>Leptodactylus ocellatus</i>	KU 289191; Paraguay: Parque Nacional San Rafael.	DQ158417	DQ158343	DQ306492
<i>Melanophryniscus stelzneri</i>	KU 289071; Paraguay : Parque Nacional San Rafael.	DQ158421	DQ158347	DQ306494
<i>Rhamphophryne festae</i>	KU 217501; Ecuador Pastaza Locacion Petrolera Garza.	DQ158423	DQ158349	DQ306521
<i>Schismaderma carens</i>	MVZ 223386; Zimbabwe: Harare.	DQ158424	DQ158350	DQ306519

**Ingroup Bufo:**

**NORTH AMERICA:**

<i>Anaxyrus americanus</i>	KU 289469; USA: Texas.	DQ158426	DQ158352	DQ306520
<i>A. boreas</i>	MVZ 223292; USA: California, Mendocino County. LSUMZ H-457; USA: Arizona: Cochise Co., Chiricahua Mts. 0.8 mi E and 1.0 mi N Portal along W side of Foot Hills Rd., USA.	DQ158498	DQ158413	DQ306499
<i>A. cognatus</i> 1	USNM 320092; USA: New Mexico.	DQ158444	DQ158367	DQ306502
<i>A. cognatus</i> 2	USNM 320116; USA: New Mexico.	TBA	TBA	DQ306498
<i>A. debilis</i> 1	MVZ 137717; USA: California, Inyo Co., Deep Springs Valley, Buckhorn Spring.	DQ158449	DQ158371	DQ306507
<i>A. exsul</i>		DQ158450	DQ158372	DQ306550

6

	ID Number; Locality	12S, tRNA <sup>val</sup> , 16S	RAG-1	CXCR-4
<i>A. fowleri</i>	USNM 314864; USA: Mississippi.	DQ158451	DQ158373	DQ306505
<i>A. microscaphus</i>	USNM 320147; USA: New Mexico.	DQ158476	DQ158395	DQ306563
<i>A. quercicus</i> 1	LSUMZ 57048; USA.	DQ158484	DQ158403	DQ306562
<i>A. quercicus</i> 2	LSUMZ H-2921; USA: Louisiana: S. Tammany Parish.	DQ158483	DQ158402	DQ306549
<i>A. terrestris</i>	LSUMZ H2904	DQ158489	TBA	DQ306537
<i>A. woodhousii</i>	KU 224658; USA: Kansas, Barber Sharon.	DQ158498	DQ158413	DQ306551
<b>North/Central America:</b>				
<i>Ollotis alvaria</i>	USNM 320001; USA: Arizona. KU 290030; El Salvador: Morazan, Perkin Lenca Hotel grounds, ca. Perquin.	DQ158425	DQ158351	DQ306516
<i>O. coccifer</i>	KU 217480; Ecuador: Pichincha, 1.0 km E Vicente Maldonado.	DQ158443	DQ158366	DQ306526
<i>O. conifera</i>	KU 289850; El Salvador: Usulután, Cerro del Tigre.	DQ158445	DQ158366	DQ306534
<i>O. luetkenii</i>	USNM 534129; Honduras: Colon.	DQ158467	DQ158387	DQ306565
<i>O. valliceps</i>		DQ158493	DQ158409	DQ306545
<b>Eurasia:</b>				
<i>Bufo andrewsi</i>	USNM 292081; China: Sichuan, Shimian.	DQ158428	DQ158353	DQ306531
<i>B. bufo</i>	MVZ 230209; Turkey: Bursa Province. FMNH 255309; Lao PDR: Champassak Prov Mounlapamok Dist., Dong Khanthung National Biodiversity Conservation Area.	DQ158438	DQ158362	DQ306504
<i>Duttaphrynus melanostictus</i>	FMNH 256443; Lao PDR: Khammouane Prov. Nakai Dist. Nakai Nam.	DQ158475	DQ158394	DQ306508
<i>Ingerophrynus galeatus</i>	FMNH 255318; Lao PDR: Champassak Prov. Mounlapamok Dist., Dong Khanthung National Biodiversity Conservation Area.	DQ158452	DQ158374	DQ306506
<i>I. macrotis</i> (Borneo)	FMNH 248148; Brunei, Belait Dist. Labi, Sg Mendaram.	DQ158468	DQ158388	DQ306525
<i>Phrynoidis asper</i>	FMNH 231245; Malaysia: Sabah, Lahad Datu Dist., Danum Valley Research Center.	DQ158431	DQ158356	--
<i>P. juxtasper</i>		DQ158463	DQ158385	DQ306542
<b>Africa:</b>				
<i>Amietophrynus brauni</i>	FMNH 251853; Tanzania: Tanga Region, Muheza Dist.	DQ158437	DQ158361	DQ306514
<i>A. camerunensis</i>	CAS 207288; Equatorial Guinea: Bioko Id.	DQ158439	DQ158363	DQ306555
<i>A. garmani</i>	CAS 214829; Kenya: Kilifi Dist., Watamu.	DQ158453	DQ158375	DQ306547
<i>A. gracilipes</i>	CAS 207620; Equatorial Guinea: Bioko Id.	DQ158456	DQ158378	DQ306522
<i>A. gutturalis</i>	CAS 214842; Kenya: Kilifi Dist., Kararacha Pond II.	DQ158460	DQ158382	DQ306556

	ID Number; Locality	12S, tRNA <sup>val</sup> , 16S	RAG-1	CXCR-4
<i>A. kisoensis</i>	CAS 202005; Uganda: Rukungiri Dist., Bwindi Impenetrable National Park.	DQ158464	--	DQ306560
<i>A. maculatus</i>	KU 290430; Ghana: Eastern Region Muni Lagoon, Winneba.	DQ158469	DQ158389	DQ306533
<i>A. poweri</i>	CAS 193885; Namibia: Okahandja.	DQ158482	DQ158401	DQ306559
<i>A. regularis</i> 2	KU 290435; Ghana Eastern Region Winneba Junction, Winneba.	DQ158485	DQ158404	DQ306523
<i>A. steindachneri</i>	CAS 214839; Kenya: Kilifi Dist., Kararacha Pond.	DQ158488	DQ158406	DQ306546
<i>A. xeros</i>	AMNH 109826; Mali: Bamako, Hotel CRES	DQ158499	DQ158414	DQ306561
<b>Caribbean:</b>				
<i>Peltophryne lemur</i>	AG (Anna Goebel); Puerto Rico	DQ158465	DQ158386	DQ306513
<b>South America:</b>				
<i>Rhinella ocellatus</i>	MZUSP 103261; Brazil: Peixe Tocantins, Brazil	DQ158479	DQ158398	DQ306538
<b><i>Rhaebo guttatus</i> group:</b>				
<i>R. glaberrimus</i> 1	QCAZ 14708; Ecuador.	DQ158454	DQ158376	DQ306510
<i>R. glaberrimus</i> 2	QCAZ 13234; Ecuador: Provincia Napo, Talag Alto.	DQ158455	DQ158377	DQ306548
<i>R. guttatus</i>	LSUMZ 17418; Brazil: Rondonia: Parque Estadual Guajara-Mirim.	DQ158459	DQ158381	DQ306497
<i>R. haematiticus</i> 1	QCAZ 13215; Ecuador: Esmeraldas, 5 km west of Durango.	DQ158461	DQ158383	DQ306501
<i>R. haematiticus</i> 2	QCAZ 17083; Provincia Esmeraldas, Alto Tambo.	DQ158435	DQ158359	DQ306558
<b><i>Rhinella granulosa</i> group:</b>				
<i>R. humboldti</i>	USNM 286986; Trinidad.	DQ158434	DQ158358	--
<i>R. granulosa</i> 1	USNM 302450; Brazil: Roraima.	DQ158457	DQ158379	DQ306557
<i>R. granulosa</i> 2	AF 0093	DQ158458	DQ158380	DQ306553
<b><i>Rhinella marinus</i> group:</b>				
<i>R. arenarum</i>	AR 305; Argentina.	DQ158429	DQ158354	DQ306529
<i>R. marinus</i> 1	KU 289750; El Salvador Ahuachapan, Parque Nacional El Imposible.	DQ158473	DQ158392	DQ306530
<i>R. marinus</i> 2	KU 217482; Ecuador: Loja, Vilcabamba.	DQ158474	DQ158393	DQ306544
<i>R. poeppigii</i>	USNM 268824; Peru: Madre de Dios.	DQ158481	DQ158400	DQ306517



7

	ID Number; Locality	12S, tRNA <sup>val</sup> , 16S	RAG-1	CXCR-4
<i>R. schneideri</i>	KU 289057; Paraguay: Parque Nacional San Luis de la Sierra.	DQ158480	DQ158399	DQ306528
<b><i>Rhinella spinulosus</i> group:</b>				
<i>R. arequipensis</i>	KU 214792; Peru: Arequipa, Arequipa Zamacola.	DQ158430	DQ158355	DQ306564
<i>R. atacamensis</i>	KU 217352; Chile: Coquimbo, Cuesta Pajonales, 117 km N La Serena.	DQ158433	DQ158357	DQ306541
<i>R. chilensis</i>	KU 217369; Chile: Santiago, 2 km S Rungue.	DQ158442	DQ158365	DQ306552
<i>R. cophotis</i>	KU 211685; Peru: Cajamarca, S slope Abra Quilsh.	DQ158446	DQ158369	DQ306540
<i>R. limensis</i>	KU 215587; Peru: Ancash, Rio Casma, 3 km ESE Casma. DLR 3837; Bolivia: Creek between Charazani and Curva, prov. Saavedra, Depto. La Paz.	DQ158466	TBA	DQ306509
<i>R. spinulosus</i>	IZUA 3198; Chile: Puerto Edén, Isla Wellington, Provincia de Mafallanes.	DQ158487	DQ158405	DQ306566
<i>R. variegatus</i>		DQ158494	DQ158410	DQ306515
<i>R. vellardi</i>	KU 211765; Peru: Cajamarca, 10 km SSE Cajabamba.	DQ158495	DQ158411	DQ306527
<b><i>Rhinella margaritifera</i> group:</b>				
<i>R. castaneoticus</i>	LSUMZ 17429; Brazil: Para: 100 km S Santarem.	DQ158440	DQ158364	DQ306539
<i>R. cf. dapsilis</i>	QCAZ 3509; Ecuador: Pichincha, Bosque Protector La Perla, 5km E La Concordia.	DQ158448	DQ158370	DQ306532
<i>R. cf. margaritifera</i> 2	QCAZ 13896; Ecuador: Cañar, Manta Real.	DQ158471	DQ158390	DQ306554
<i>R. cf. margaritifera</i> 3	QCAZ 11597; Ecuador: Provincia Esmeraldas, Bosque Protector, 30 km from San Lorenz by way of Ibarra.	DQ158472	DQ158391	DQ306543
<i>R. cf. margaritifera</i> 4	USNM 268828; Peru: Madre de Dios.	DQ158490	DQ158407	DQ306518
<i>R. cf. margaritifera</i> 5	KU 215145; Peru: Madre de Dios.	DQ158491	--	DQ306511
<i>R. nasicus</i>	ROM 20560; Guyana: Mazaruni-Potaro District, Potaro River, Tukeit.	DQ158477	DQ158396	DQ306512
<b><i>Rhinella veraguensis</i> group:</b>				
<i>R. amboroensis</i>	DLR 3888; Bolivia: Río Chua Khocha, La Siberia, prov.. Carrasco, Depto.. Cochabamba.			
<i>R. nesiotas</i>	UTA 53310; Bolivia: La Paz, Caranavi: Serranía de Bella Vista.	DQ158478	DQ158397	DQ306500
<i>R. veraguensis</i> 1	DLR 3820; Bolivia: Serranía Bellavista, prov. Noryungas, Depto. La Paz.	DQ158496	DQ158412	DQ306524
<i>R. veraguensis</i> 2	USNM 346048; Peru: Cuzco.	DQ158497	TBA	DQ306535

8

9